

## Inesite, a hydrated calcium manganese silicate with five-tetrahedral-repeat double chains

CHE'NG WAN AND SUBRATA GHOSE

Department of Geological Sciences  
University of Washington  
Seattle, Washington 98915

### Abstract

Inesite,  $\text{Ca}_2\text{Mn}_7\text{Si}_{10}\text{O}_{28}(\text{OH})_2 \cdot 5\text{H}_2\text{O}$ , from the Hale Creek Mine, Trinity County, California, is triclinic, space group  $PT$ , with cell dimensions  $a = 8.889(2)$ ,  $b = 9.247(2)$ ,  $c = 11.975(3)\text{Å}$ ;  $\alpha = 88.15(2)$ ,  $\beta = 132.07(2)$  and  $\gamma = 96.64(2)^\circ$ ;  $Z = 1$ . The crystal structure has been determined through a combination of the three-dimensional Patterson and the symbolic addition methods. The structure has been refined by the method of least squares to an  $R$  factor of 0.032 for 4243 reflections.

The crystal structure of inesite consists of two components: (a) a polyhedral band, consisting of a sequence of seven edge-sharing Mn octahedra and two Ca pentagonal bipyramids, connected to two similar sequences on either side by edge-sharing; and (b) double silicate chains with a five-tetrahedral-repeat period, which contain alternating six- and eight-membered rings. These silicate double chains knit the adjacent Ca, Mn polyhedral bands into a three-dimensional framework. The average Ca-O distance is 2.431Å. The average Mn-O distances within the four different Mn octahedra are 2.243, 2.217, 2.218 and 2.210Å. The three crystallographically independent water molecules serve as apical ligands to the Ca and Mn atoms. The site of one of the water molecules is statistically occupied half the time, accounting for five water molecules in the unit cell. All seven hydrogen atoms are involved in hydrogen bonding. The recipient of a hydrogen bond is either a water molecule or a bridging oxygen atom bonded to two silicon only. The average Si-O bond lengths within the five different Si tetrahedra are 1.621, 1.626, 1.623, 1.627 and 1.630Å. The Si-O-Si angles range from  $130.0^\circ$  to  $143.5^\circ$ , the smaller Si-O-Si angles being associated with longer Si-O bonds and *vice versa*. The six- and eight-membered silicate rings are nearly planar.

The oriented thermal transformation of inesite to a high-calcium rhodonite at  $\sim 800^\circ\text{C}$  involves considerable cation migration and breakage of Si-O bonds and is far from a simple dehydration reaction, as has been postulated.

### Introduction

Single silicate chains with two-, three-, four-, five-, six-, seven-, nine-, and twelve-tetrahedral repeat are known (Liebau, 1972). These single chains can polymerize further to form double chains. A common example is the polymerization of pyroxene-type (two-tetrahedral repeat) chains into amphibole-type double chains. Likewise, wollastonite-type (three-tetrahedral repeat) single chains can polymerize into xonotlite-type double chains. However, silicate double chains with periodicities of five and seven tetrahedra have not been reported. The crystal structure of inesite provides the first example of double silicate chains with a periodicity of five tetrahedra (*Fünfer-Doppelketten*) (Wan and Ghose, 1975).

### Previous work

Inesite, a hydrated calcium manganese silicate, is triclinic, crystal class  $\bar{1}$ . From chemical analysis of inesite from Quinault, Washington, Glass and Schaller (1939) suggested the chemical formula  $3\text{CaO} \cdot 11\text{MnO} \cdot 15\text{SiO}_2 \cdot 10\text{H}_2\text{O}$ . Richmond (1942) determined the correct chemical composition as  $\text{Ca}_2\text{Mn}_7\text{Si}_{10}\text{O}_{28}(\text{OH})_2 \cdot 5\text{H}_2\text{O}$ , and assigned inesite to the rhodonite group of pyroxenoids on the basis of its cleavage characteristics and unit-cell dimensions. The similarity of the  $c$  cell dimensions ( $\sim 12.20\text{Å}$ ) between rhodonite and inesite led Liebau (1956) to postulate the presence of a silicate chain with five-tetrahedral repeat in inesite by analogy with rhodonite; Liebau further speculated that since inesite is hydrated (*cf.*

Table 1. Crystal data

Inesite. Hale Creek Mine, Trinity County, California	
Flesh-red transparent short prisms	
NMNH # 127455	
Triclinic, $\bar{1}$	
$a$ (Å): 8.889(2)	Space group: $P\bar{1}$
$b$ (Å): 9.247(2)	Cell volume (Å <sup>3</sup> ): 724.4(3)
$c$ (Å): 11.975(3)	Cell content: $[\text{Ca}_2\text{Mn}_7\text{Si}_{10}\text{O}_{28}(\text{OH})_2 \cdot 5\text{H}_2\text{O}]$
$\alpha$ (°): 88.15(2)	$D_m$ : 3.03 g cm <sup>-3</sup>
$\beta$ (°): 132.07(2)	$D_o$ : 3.03 g cm <sup>-3</sup>
$\gamma$ (°): 96.64(2)	$\mu$ (MoK $\alpha$ ): 39.80 cm <sup>-1</sup>

amphiboles and xonotlite), it might contain double chains rather than single chains. On the basis of infrared absorption spectra of pyroxenoids, including inesite, Ryall and Threadgold (1966) concluded that inesite contains a single silicate chain with five-tetrahedral repeat.

### Experimental

A transparent cleavage fragment of inesite with dimensions  $0.12 \times 0.12 \times 0.20$  mm from Crescent Mine, Olympic Peninsula, Washington, was used initially for the structure determination. The unit-cell dimensions were refined from 15 reflections with  $2\theta$  values between 40 and 50°, measured with MoK $\alpha$  radiation on an automatic single-crystal diffractometer. These dimensions [ $a = 8.862(2)$ ,  $b = 9.258(2)$ ,  $c = 11.972(2)$  Å,  $\alpha = 88.08(1)^\circ$ ,  $\beta = 132.02(1)^\circ$  and  $\gamma = 96.77(1)^\circ$ ; cell volume 723.3(3) Å<sup>3</sup>] are in good agreement with those determined under similar experimental conditions on a sample of inesite from the Hale Creek Mine, Trinity County, California (Table 1). Both these sets of cell dimensions are in fair agreement with those determined by Richmond (1942) on an inesite sample from Quinault, Washington.

The unit cell chosen here is not a reduced cell. This non-conventional choice follows Richmond (1942), who chose this orientation to make the elongation of the cleavage fragments the direction of the  $c$  axis; furthermore, the two perfect cleavages were taken as {100} and {010}, which correspond to those of a number of pyroxenoids (e.g., wollastonite, rhodonite, etc.). This choice also facilitates a comparison of the inesite structure with that of rhodonite, since these two minerals are chemically and structurally closely related.

A first set of 1453 reflections were measured on the

inesite sample from Crescent Mine, Washington on an automatic single-crystal diffractometer (Syntex P1) using the  $2\theta-\theta$  scan method. MoK $\alpha$  radiation, monochromatized by reflection from a "single" crystal of graphite, and a scintillation counter were used for the measurements. The reflection intensities were corrected for Lorentz and polarization factors, but not for absorption.

An inesite sample from Trinity County, California was used for the measurement of a second data set. An approximate sphere with a diameter of 0.25(2) mm was ground in a sphere grinder (Bond, 1951) from a clear transparent cleavage fragment. This data set was collected on the same diffractometer under similar conditions. The variable scan method was used, the minimum scan rate being 2°/min (50 kV, 10 mA). All reflections within  $2\theta$  values  $\leq 60^\circ$  were measured—a total of 4243 reflections, out of which 532 were below  $3\sigma(I)$ , where  $\sigma(I)$  is the standard deviation of the intensity,  $I$ , as determined from the counting statistics. These data were corrected for Lorentz, polarization, and absorption factors and were used for the final refinement of the structure.

### Determination and refinement of the structure

The first data set was used for the structure determination. Wilson statistics of the reflection intensities indicated the presence of a center of symmetry, and fixed the space group of inesite as  $P\bar{1}$ . Since inesite contains seven Mn atoms in the unit cell, one Mn atom must be on a symmetry center. Mn(1) was arbitrarily chosen to be at the origin (0,0,0). Hence, in the three-dimensional Patterson map, an image of the structure exists in its true position, modulated by the electron density of Mn(1). The atomic positions of Mn(2), Mn(3), and Mn(4) were retrieved by systematically considering Mn(1)–Mn( $i$ ) vectors ( $x_i, y_i, z_i$ ), which occur halfway between Mn( $i$ )–Mn( $i$ ) vectors ( $2x_i, 2y_i, 2z_i$ ) from manganese atoms in general positions related by the center of inversion. These manganese positions were confirmed by considering interatomic vectors between crystallographically different manganese atoms ( $x_i - x_j, y_i - y_j, z_i - z_j$ ). The first structure-factor calculation with four manganese atoms yielded an  $R$  factor of 0.71. A Fourier synthesis revealed the positions of the calcium, four silicon, and twelve oxygen atoms.

Simultaneously, an attempt was made to determine the structure directly by the symbolic addition method (Karle and Karle, 1966).  $E$  values for all reflections were calculated. 241 reflections showed  $E$  values  $\geq 2.0$ . The signs of the three following reflec-

tions were chosen to define the origin:

<i>h</i>	<i>k</i>	<i>l</i>	<i>E</i>	Sign
8	3	0	6.20	—
0	6	3	4.27	—
1	0	$\bar{4}$	4.07	+

Programs SIGMA 2 and PHASE incorporated in the X-RAY SYSTEM-70 (Stewart *et al.*, 1972) were used for the phase determination. In addition to the signs of the three origin-determining reflections, the sign of the reflection (30 $\bar{3}$ ) (*E* value 3.64) was alternately chosen as + and —, yielding two sets of signs, A and B. For the set A, 91 were “+” and 86 “—”, and for the set B, 84 “+” and 93 “—”. The *E* map, calculated from the signs of set B, showed atomic positions comparable to those found from the Patterson map, except that they were shifted by the translation  $\mathbf{b}/2 + \mathbf{c}/2$ . The positions of the calcium, four manganese, four silicon, and seven oxygen atoms found from the *E* map were adjusted to conform to those found from the Patterson map. Now the signs of all 177 reflections, whose signs were defined, turned out to be “+”. Positions of the remaining non-hydrogen atoms (one silicon and eleven oxygen atoms) were determined from Fourier and difference Fourier syntheses.

Based on the first data set, the structure was refined by the method of least squares with isotropic temperature factors, using Finger's (1968) RFINE program. The temperature factor of O(W3) was unusually high. The occupancy of O(W3) was refined and found to be 0.49. The final *R* factor was 0.060 for 1453 reflections. Based on the second data set, the atomic positions of the non-hydrogen atoms were refined first by the method of least squares using anisotropic temperature factors to an *R* factor of 0.045. A difference Fourier synthesis subsequently indicated the positions of all the hydrogen atoms, including those attached to O(W3). Although all the hydrogen atoms found were stereochemically reasonable, an attempt to refine their positions using isotropic temperature factors was only partially successful. For subsequent refinement, the isotropic temperature factors, B, for all hydrogen atoms were fixed at 4.0. The occupancies of the oxygen atom O(W3) and the two hydrogen atoms attached to O(W3) were fixed at 0.5. Because the dimensions were too large, the least-squares refinement was carried out in blocks, using the least-squares refinement program incorporated in the X-RAY SYSTEM-72 (Stewart *et al.*, 1972). Each atom was assigned one block, except the (OH) group and the water molecules, which were assigned one block each.

The scattering factors for Ca, Mn, Si, O, and H were taken from Cromer and Mann (1968) and corrected for anomalous dispersion (Cromer and Liberman, 1970). At the final stages of the refinement, the occupancy of O(W3) was refined and found to be 0.478(6). The final *R* factor for 4243 reflections is 0.032. The atomic positional and thermal parameters are listed in Table 2. Since the hydrogen positions could not be refined, they should be considered tentative: The observed and calculated structure factors are compared in Table 3.<sup>1</sup> Table 4 lists the bond lengths and angles with their standard deviations, which include the standard deviation of the measured unit-cell dimensions. The average standard deviations in Ca—O, Mn—O, and Si—O bond lengths are 0.003, 0.002 and 0.003Å respectively, whereas those in O—Ca—O, O—Mn—O and O—Si—O angles are all 0.1°.

### Description of the structure

The crystal structure of inesite is a three-dimensional framework composed of two components:

- polyhedral bands consisting of four different types of Mn octahedra and a Ca pentagonal bipyramid, and
- single silicate chains with five-tetrahedral repeat, polymerized into double chains with alternating six- and eight-membered rings (*Fünfer-Doppelketten*).

#### The Ca and Mn polyhedra

The [CaO<sub>5</sub>(OH)(H<sub>2</sub>O)] polyhedron is a distorted pentagonal bipyramid. The Ca—O bond distances range from 2.278 to 2.823Å, the average being 2.431Å.

The four crystallographically-distinct Mn octahedra are nearly regular; the average Mn—O bond distances within the [Mn(1)O<sub>4</sub>(OH)<sub>2</sub>], [Mn(2)O<sub>6</sub>], [Mn(3)O<sub>5</sub>(H<sub>2</sub>O)] and [Mn(4)O<sub>4</sub>(OH)(H<sub>2</sub>O)] octahedra are 2.243, 2.217, 2.218 and 2.210Å respectively. The site of the water molecule, W(3), which serves as the apical ligand to Mn(4), is statistically occupied half the time. W(3) is separated from its centrosymmetric equivalent by 1.918Å; thus, when the Mn(4) octahedron has its apical position occupied by H<sub>2</sub>O, the centrosymmetrically-related Mn(4) octahedron must have its corresponding apical position vacant.

<sup>1</sup> To obtain a copy of Table 3, order Document No. AM-78-070 from the Business Office, Mineralogical Society of America, LL 1000, 1909 K Street, NW, Washington, DC 20006. Please remit \$1.00 in advance for the microfiche.

Table 2a. Inesite: positional and thermal parameters of non-hydrogen atoms (standard deviations in parentheses)

Atom	x	y	z	$u_{11}^*$	$u_{22}$	$u_{33}$	$u_{12}$	$u_{13}$	$u_{23}$
Ca	0.38823(9)	0.26154(6)	0.10164(6)	205(3)	120(2)	75(2)	42(2)	73(2)	7(2)
Mn(1)	0.00000	0.00000	0.00000	111(3)	139(3)	84(2)	13(2)	66(2)	7(2)
Mn(2)	0.09978(6)	0.07665(4)	0.77404(4)	93(2)	96(2)	83(2)	16(1)	66(2)	6(1)
Mn(3)	0.20633(6)	0.11273(4)	0.55863(4)	86(2)	124(2)	86(2)	8(1)	65(2)	1(1)
Mn(4)	0.30756(6)	0.15973	0.33874(4)	87(2)	218(2)	85(2)	0(2)	66(2)	3(2)
Si(1)	0.13271(10)	0.72738(7)	0.77309(7)	76(3)	77(3)	65(3)	9(2)	56(3)	4(2)
Si(2)	0.21219(11)	0.75524(8)	0.55699(8)	83(3)	90(3)	81(3)	12(2)	66(3)	5(2)
Si(3)	0.01735(11)	0.60119(8)	0.26428(8)	109(3)	80(3)	87(3)	4(2)	79(3)	4(2)
Si(4)	0.31748(11)	0.81419(3)	0.28134(8)	69(3)	103(3)	71(3)	11(2)	52(3)	12(2)
Si(5)	0.40405(10)	0.88778(8)	0.08109(7)	69(3)	97(3)	60(3)	13(2)	49(3)	5(2)
O(1)	0.6530(3)	0.2168(2)	0.0560(2)	92(8)	124(8)	78(8)	18(7)	55(7)	-6(6)
O(2)	0.9568(3)	0.4283(2)	0.2119(2)	204(10)	74(8)	167(9)	-14(7)	156(9)	-9(7)
O(3)	0.0265(3)	0.1558(2)	0.3087(2)	84(3)	107(8)	106(8)	28(6)	69(7)	18(6)
O(4)	0.7920(3)	0.3069(2)	0.3140(2)	154(9)	153(9)	99(8)	52(7)	106(8)	32(7)
O(5)	0.9267(3)	0.1140(2)	0.5295(2)	102(8)	110(8)	103(8)	20(7)	76(7)	17(6)
O(6)	0.8988(3)	0.3865(2)	0.5653(2)	221(10)	113(9)	114(9)	8(7)	128(8)	-3(7)
O(7)	0.5515(3)	0.2071(2)	0.3509(2)	112(9)	229(10)	189(10)	17(8)	111(8)	35(8)
O(8)	0.1636(3)	0.3038(2)	0.8471(2)	116(9)	127(9)	144(9)	36(7)	79(8)	6(7)
O(9)	0.7826(3)	0.3452(2)	0.7148(2)	135(9)	108(8)	192(9)	7(7)	133(8)	29(7)
O(10)	0.8280(3)	0.0630(2)	0.7639(2)	98(8)	126(8)	121(9)	27(7)	80(8)	11(7)
O(11)	0.6840(3)	0.2144(2)	0.8542(2)	-29(9)	147(9)	117(8)	-5(7)	103(8)	8(7)
O(12)	0.4512(3)	0.1449(2)	0.5644(2)	75(8)	228(10)	89(8)	3(7)	58(7)	1(7)
O(13)	0.2728(3)	0.0236(2)	0.0080(2)	123(9)	127(9)	105(8)	43(7)	81(8)	19(7)
O(14)	0.3535(3)	0.0736(2)	0.7880(2)	71(8)	167(9)	92(8)	15(7)	58(7)	7(7)
O(OH)	0.1332(3)	0.2161(2)	0.1074(2)	133(9)	167(9)	137(9)	43(7)	98(8)	21(7)
O(W1)	0.2640(4)	0.3600(3)	0.5957(3)	222(12)	174(11)	287(12)	31(9)	100(10)	-8(9)
O(W2)	0.5498(7)	0.4905(4)	0.8799(3)	1407(40)	357(19)	220(16)	439(23)	-72(20)	-54(14)
O(W3)	0.4024(7)	0.4159(5)	0.4399(5)	234(23)	232(23)	315(25)	102(19)	153(21)	132(19)

\*Anisotropic Temperature factors ( $\times 10^4$ )  $\exp[-2\pi^2(u_{11}^2 a^{*2} + u_{22}^2 b^{*2} + u_{33}^2 c^{*2} + 2u_{12}^* hka^*b^* \cos \gamma + 2u_{13}^* hla^*c^* \cos \beta + 2u_{23}^* klb^*c^* \cos \alpha^*)]$ .

Table 2b. Inesite: positional parameters of the hydrogen atoms

Atom	x	y	z
H(1)	0.025	0.281	0.064
H(2)	0.127	0.373	0.528
H(3)	0.315	0.379	0.544
H(4)	0.640	0.433	0.950
H(5)	0.483	0.433	0.788
H(6)	0.553	0.413	0.527
H(7)	0.348	0.466	0.363

### The polyhedral band

The polyhedral band is composed of a sequence of seven edge-sharing Mn octahedra; the Mn(1) octahedron occurs at the center and one Ca polyhedron occurs at each end of this sequence. This band, consisting of nine polyhedra, is connected to two identical sequences on either side in a staggered fashion, giving rise to a serrated polyhedral band. The chain offset occurs at Mn(1), which is flanked on either side by Ca polyhedra (Fig. 1).

### The double silicate chains

A single silicate chain with five-tetrahedral repeat is connected to a centrosymmetrically equivalent

chain by corner-sharing, thereby forming a double chain (*Fünfer-Doppelkette*). This double chain contains alternating six- and eight-membered rings (Fig. 2). These two ring systems have Si(1) and Si(3) tetrahedra in common. In contrast, the amphibole-type double chain contains only six-membered rings, whereas xonotlite contains only eight-membered rings (Mamedov and Belov, 1956).

### The three-dimensional framework

The packing of the polyhedral bands and the silicate double chains in inesite is very different from that found in pyroxenes, pyroxenoids, and amphiboles (*cf.* Prewitt and Peacor, 1964). The structural scheme of inesite is shown in Figure 3, where two adjacent polyhedral bands are connected together by a double-silicate chain, sharing tetrahedral and octahedral corners. In addition, two tetrahedral edges [O(1)-O(4) and O(4)-O(7)] belonging to the Si(1) and Si(2) tetrahedra are shared with the Ca polyhedron. At this level, inesite can be considered as an imperfect but densely packed layer structure, with alternating octahedral and tetrahedral bands within each layer.

Table 4. Inesite: interatomic distances (Å) and angles (°) (standard deviations in parentheses)

The Ca Polyhedron				The Mn(4) Octahedron			
Ca - 0(1)	2.823(3)	0(1) - Ca - 0(4)	55.77(8)	Mn(4) - 0(3)	2.269(3)	0(3) - Mn(4) - 0(12)	82.24(9)
Ca - 0(4)	2.649(2)	0(1) - Ca - 0(7)	107.57(8)	Mn(4) - 0(7)	2.068(3)	0(3) - Mn(4) - 0(OH)	90.23(10)
Ca - 0(7)	2.352(3)	0(1) - Ca - 0(13)	80.17(9)	Mn(4) - 0(12)	2.084(2)	0(3) - Mn(4) - 0(W3)	87.34(18)
Ca - 0(13)	2.290(2)	0(1) - Ca - 0(OH)	160.33(7)	Mn(4) - 0(OH)	2.165(2)	0(3) - Mn(4) - 0(10)	83.01(9)
Ca - 0(OH)	2.304(3)	0(1) - Ca - 0(8)	83.77(9)	Mn(4) - 0(W3)	2.478(5)	0(7) - Mn(4) - 0(12)	102.63(9)
Ca - 0(8)	2.319(2)	0(1) - Ca - 0(W2)	95.03(19)	Mn(4) - 0(10)	2.193(2)	0(7) - Mn(4) - 0(OH)	82.92(10)
Ca - 0(W2)	2.278(4)	0(4) - Ca - 0(7)	60.44(9)	Mean	2.210	0(7) - Mn(4) - 0(W3)	83.38(19)
Mean	2.431	0(4) - Ca - 0(13)	111.72(7)			0(7) - Mn(4) - 0(10)	105.87(11)
		0(4) - Ca - 0(OH)	133.38(9)	0(3) - 0(12)	2.866(2)	0(12) - Mn(4) - 0(W3)	75.12(15)
0(1) - 0(4)	2.564(4)	0(4) - Ca - 0(8)	131.82(10)	0(3) - 0(OH)	3.142(4)	0(12) - Mn(4) - 0(10)	105.66(8)
0(1) - 0(13)	2.663(3)	0(4) - Ca - 0(W2)	78.11(12)	0(3) - 0(W3)	3.281(6)	0(OH) - Mn(4) - 0(W3)	94.52(14)
0(1) - 0(8)	3.454(3)	0(7) - Ca - 0(13)	95.01(8)	0(3) - 0(10)	2.957(4)	0(OH) - Mn(4) - 0(10)	83.30(8)
0(4) - 0(7)	2.530(4)	0(7) - Ca - 0(OH)	74.03(9)	0(7) - 0(12)	3.241(5)	Mean	89.69
0(4) - 0(W2)	3.117(5)	0(7) - Ca - 0(8)	167.64(11)	0(1) - 0(OH)	2.804(3)		
0(7) - 0(13)	3.423(3)	0(7) - Ca - 0(W2)	102.35(11)	0(7) - 0(W3)	3.039(8)	0(3) - Mn(4) - 0(7)	167.97(8)
0(7) - 0(OH)	2.804(3)	0(13) - Ca - 0(OH)	80.16(9)	0(7) - 0(10)	3.401(3)	0(12) - Mn(4) - 0(OH)	167.39(10)
0(13) - 0(OH)	2.958(4)	0(13) - Ca - 0(8)	81.86(7)	0(12) - 0(W3)	2.799(6)	0(W3) - Mn(4) - 0(10)	170.09(17)
0(13) - 0(8)	3.020(3)	0(13) - Ca - 0(W2)	162.23(11)	0(12) - 0(10)	3.409(3)		
0(OH) - 0(8)	3.371(4)	0(OH) - Ca - 0(8)	93.63(9)	0(OH) - 0(W3)	3.417(6)		
0(8) - 0(W2)	3.434(7)	0(OH) - Ca - 0(W2)	103.84(19)	0(OH) - 0(10)	2.896(3)		
		0(8) - Ca - 0(W2)	81.02(9)	Mean	3.104		
The Mn(1) Octahedron				The Si(1) Tetrahedron			
Mn(1) - 0(13)	2.346(3) (x2)	0(13) - Mn(1) - 0(OH)	82.13(10) (x2)	Si(1) - 0(1)	1.634(2)	0(1) - Si(1) - 0(2)	106.5(1)
Mn(1) - 0(OH)	2.151(2) (x2)	0(13) - Mn(1) - 0(10)	82.33(8) (x2)	Si(1) - 0(2)	1.627(2)	0(1) - Si(1) - 0(4)	103.4(1)
Mn(1) - 0(10)	2.231(2) (x2)	0(OH) - Mn(1) - 0(10)	82.73(8) (x2)	Si(1) - 0(4)	1.625(3)	0(1) - Si(1) - 0(3)	113.6(1)
Mean	2.243	0(13) - Mn(1) - 0(OH) <sup>†</sup>	97.87(10) (x2)	Si(1) - 0(3)	1.599(2)	0(2) - Si(1) - 0(4)	107.0(1)
		0(13) - Mn(1) - 0(10) <sup>†</sup>	97.67(8) (x2)	Mean	1.621	0(2) - Si(1) - 0(3)	113.6(1)
0(13) - 0(OH)	2.958(4) (x2)	0(OH) - Mn(1) - 0(10) <sup>†</sup>	97.27(8) (x2)			0(4) - Si(1) - 0(3)	112.1(1)
0(13) - 0(10)	3.014(3) (x2)	Mean	90.00	0(1) - 0(2)	2.620(3)	Mean	109.4
0(13) - 0(OH) <sup>†</sup>	3.393(3) (x2)			0(1) - 0(4)	2.564(4)		
0(13) - 0(10) <sup>†</sup>	3.446(4) (x2)			0(1) - 0(3)	2.712(2)		
0(OH) - 0(10)	2.896(3) (x2)			0(2) - 0(4)	2.614(4)		
0(OH) - 0(10) <sup>†</sup>	3.289(3) (x2)			0(2) - 0(3)	2.699(3)		
Mean	3.166			0(4) - 0(3)	2.675(4)		
				Mean	2.647		
The Mn(2) Octahedron				The Si(2) Tetrahedron			
Mn(2) - 0(8)	2.163(2)	0(8) - Mn(2) - 0(14)	96.86(9)	Si(2) - 0(4)	1.653(3)	0(4) - Si(2) - 0(5)	111.8(2)
Mn(2) - 0(14)	2.151(3)	0(8) - Mn(2) - 0(13)	88.03(8)	Si(2) - 0(5)	1.616(2)	0(4) - Si(2) - 0(6)	102.6(1)
Mn(2) - 0(13)	2.183(2)	0(8) - Mn(2) - 0(5)	96.27(8)	Si(2) - 0(6)	1.651(2)	0(4) - Si(2) - 0(7)	102.9(1)
Mn(2) - 0(5)	2.254(2)	0(8) - Mn(2) - 0(10)	86.54(9)	Si(2) - 0(7)	1.582(2)	0(5) - Si(2) - 0(6)	107.7(1)
Mn(2) - 0(10)	2.325(3)	0(14) - Mn(2) - 0(13)	94.01(9)	Mean	1.626	0(5) - Si(2) - 0(7)	116.9(1)
Mn(2) - 0(3)	2.225(2)	0(14) - Mn(2) - 0(5)	83.53(9)			0(6) - Si(2) - 0(7)	114.0(2)
Mean	2.217	0(14) - Mn(2) - 0(3)	95.60(9)			Mean	109.3
		0(13) - Mn(2) - 0(10)	83.86(9)	0(4) - 0(5)	2.708(3)		
0(8) - 0(14)	3.227(4)	0(13) - Mn(2) - 0(3)	92.13(7)	0(4) - 0(6)	2.579(4)		
0(8) - 0(13)	3.020(3)	0(5) - Mn(2) - 0(10)	98.26(9)	0(4) - 0(7)	2.530(4)		
0(8) - 0(5)	3.290(3)	0(5) - Mn(2) - 0(3)	84.09(7)	0(5) - 0(6)	2.637(3)		
0(8) - 0(10)	3.078(3)	0(10) - Mn(2) - 0(3)	81.05(9)	0(5) - 0(7)	2.725(3)		
0(8) - 0(13)	3.169(4)	Mean	90.03	0(6) - 0(7)	2.710(3)		
0(14) - 0(5)	2.937(2)			Mean	2.648		
0(14) - 0(3)	3.242(3)	0(8) - Mn(2) - 0(3)	167.50(11)				
0(13) - 0(10)	3.014(3)	0(14) - Mn(2) - 0(10)	179.93(7)				
0(13) - 0(3)	3.175(3)	0(13) - Mn(2) - 0(5)	175.31(9)				
0(5) - 0(10)	3.463(4)						
0(5) - 0(3)	3.000(3)						
0(10) - 0(3)	2.957(4)						
Mean	3.131						
The Mn(3) Octahedron				The Si(3) Tetrahedron			
Mn(3) - 0(3)	2.309(2)	0(3) - Mn(3) - 0(12)	80.60(9)	Si(3) - 0(2)	1.629(2)	0(2) - Si(3) - 0(6)	106.9(1)
Mn(3) - 0(12)	2.117(3)	0(3) - Mn(3) - 0(W1)	85.10(9)	Si(3) - 0(6)	1.640(3)	0(2) - Si(3) - 0(9)	106.0(2)
Mn(3) - 0(14)	2.149(2)	0(3) - Mn(3) - 0(5)	92.50(9)	Si(3) - 0(9)	1.636(3)	0(2) - Si(3) - 0(8)	114.0(1)
Mn(3) - 0(W1)	2.275(2)	0(3) - Mn(3) - 0(5) <sup>†</sup>	83.55(7)	Si(3) - 0(8)	1.585(2)	0(6) - Si(3) - 0(9)	105.0(1)
Mn(3) - 0(5)	2.268(3)	0(12) - Mn(3) - 0(14)	103.55(9)	Mean	1.623	0(6) - Si(3) - 0(8)	111.6(2)
Mn(3) - 0(5) <sup>†</sup>	2.192(2)	0(12) - Mn(3) - 0(W1)	83.19(11)			0(9) - Si(3) - 0(8)	112.7(1)
Mean	2.218	0(12) - Mn(3) - 0(5) <sup>†</sup>	104.01(10)			Mean	109.4
		0(14) - Mn(3) - 0(W1)	94.66(9)	0(2) - 0(6)	2.626(3)		
0(3) - 0(12)	2.866(2)	0(14) - Mn(3) - 0(5)	83.32(9)	0(2) - 0(9)	2.607(3)		
0(3) - 0(W1)	3.100(3)	0(14) - Mn(3) - 0(5) <sup>†</sup>	95.99(8)	0(2) - 0(8)	2.696(3)		
0(3) - 0(5)	3.306(4)	0(W1) - Mn(3) - 0(5)	89.02(11)	0(6) - 0(9)	2.600(5)		
0(3) - 0(5) <sup>†</sup>	3.000(3)	0(5) - Mn(3) - 0(5) <sup>†</sup>	82.24(9)	0(6) - 0(8)	2.668(3)		
0(12) - 0(14)	3.351(4)	Mean	89.81	0(9) - 0(8)	2.682(3)		
0(12) - 0(W1)	2.918(4)			Mean	2.647		
0(12) - 0(5) <sup>†</sup>	3.396(3)	0(3) - Mn(3) - 0(14)	175.80(10)				
0(14) - 0(W1)	3.254(3)	0(12) - Mn(3) - 0(5)	169.97(7)				
0(14) - 0(5)	2.937(2)	0(16) - Mn(3) - 0(5) <sup>†</sup>	165.34(7)				
0(14) - 0(5) <sup>†</sup>	3.226(3)						
0(W1) - 0(5)	3.185(4)						
0(5) - 0(5) <sup>†</sup>	2.934(4)						
Mean	3.123						
				The Si(4) Tetrahedron			
				Si(4) - 0(9)	1.647(2)	0(9) - Si(4) - 0(10)	109.9(1)
				Si(4) - 0(10)	1.618(2)	0(9) - Si(4) - 0(11)	102.7(1)
				Si(4) - 0(11)	1.644(3)	0(9) - Si(4) - 0(12)	111.4(1)
				Si(4) - 0(12)	1.600(2)	0(10) - Si(4) - 0(11)	110.0(1)
				Mean	1.627	0(10) - Si(4) - 0(12)	113.6(1)
						0(11) - Si(4) - 0(12)	108.7(2)
						Mean	109.4
				0(9) - 0(10)	2.673(3)		
				0(9) - 0(11)	2.570(4)		
				0(9) - 0(12)	2.683(3)		
				0(10) - 0(11)	2.671(4)		
				0(10) - 0(12)	2.692(3)		
				0(11) - 0(12)	2.636(3)		
				Mean	2.654		

Table 4. (Continued)

The Si(5)		Tetrahedron	
Si(5) - O(13)	1.614(2)	O(13) - Si(5) - O(11)	106.7(2)
Si(5) - O(11)	1.644(3)	O(13) - Si(5) - O(14)	116.7(1)
Si(5) - O(14)	1.600(2)	O(13) - Si(5) - O(1)	108.8(1)
Si(5) - O(1)	1.662(3)	O(11) - Si(5) - O(14)	109.5(1)
Mean	1.630	O(11) - Si(5) - O(1)	104.4(1)
		O(14) - Si(5) - O(1)	110.1(1)
		Mean	109.4
O(13) - O(11)	2.613(3)		
O(13) - O(14)	2.736(3)		
O(13) - O(1)	2.663(3)		
O(11) - O(14)	2.649(4)		
O(11) - O(1)	2.611(4)		
O(14) - O(1)	2.675(2)		
Mean	2.658		
<i>Cation-cation distances</i>		<i>Si - O - Si angles</i>	
Si(1) - Si(2)	3.103(2)	Si(1) - O(4) - Si(2)	142.3(1)
Si(2) - Si(3)	2.989(2)	Si(2) - O(6) - Si(3)	130.5(2)
Si(3) - Si(1)	3.092(1)	Si(3) - O(2) - Si(1)	143.5(2)
Si(3) - Si(4)	3.020(2)	Si(3) - O(9) - Si(4)	133.8(2)
Si(4) - Si(5)	3.009(2)	Si(4) - O(11) - Si(5)	132.5(1)
Si(5) - Si(1)	3.037(1)	Si(5) - O(1) - Si(1)	133.6(2)
Ca - Mn(1)	3.446(1)		
Ca - Mn(2)	3.290(1)		
Ca - Mn(4)	3.444(1)		
Mn(1) - Mn(2)	3.400(1)		
Mn(1) - Mn(4)	3.271(1)		
Mn(2) - Mn(3)	3.288(1)		
Mn(2) - Mn(3)	3.341(1)		
Mn(2) - Mn(4)	3.94(1)		
Mn(3) - Mn(4)	3.308(1)		
<i>HYDROGEN BONDS</i>			
<i>The hydroxyl group</i>			
H(1) - (OH)	1.00	(OH) - H(1)...O(11)	123
H(1) - O(11)	2.31	Ca - (OH) - H(1)	123
(OH) - O(11)	2.984(3)	Mn(1) - (OH) - H(1)	111
		Mn(4) - (OH) - H(1)	118
<i>The water molecule, W(1)</i>			
W(1) - H(2)	0.93	H(2) - W(1) - H(3)	108
W(1) - H(3)	0.99	W(1) - H(2)...O(4)	152
H(2) - O(4)	2.29	W(1) - H(3)...W(3)	178
W(1) - O(4)	3.144(3)	Mn(3) - W(1) - H(2)	95
H(3) - W(3)	1.83	Mn(3) - W(1) - H(3)	97
W(1) - W(2)	2.731(4)		
<i>The water molecule, W(2)</i>			
W(2) - H(4)	0.89	H(4) - W(2) - H(5)	102
W(2) - H(5)	0.97	W(2) - H(4)...O(1)	141
H(4) - O(1)	2.31	W(2) - H(4)...O(2)	144
H(4) - O(2)	2.44	W(2) - H(5)...W(1)	155
W(2) - O(1)	3.049(4)	Ca - W(2) - H(4)	124
W(2) - O(2)	3.207(4)	Ca - W(2) - H(5)	123
H(5) - W(1)	1.83		
<i>The water molecule, W(3)</i>			
W(3) - H(6)	1.01	H(6) - W(3) - H(7)	126
W(3) - H(7)	0.85	W(3) - H(7)...O(9')	138
W(3) - O(9)	2.855(4)	W(3) - H(6)...O(9)	153
H(6) - O(9)	1.92	Mn(4) - W(3) - H(6)	99
H(7) - O(9')	2.05	Mn(4) - W(3) - H(7)	104
W(3) - O(9')	2.741(5)		

### Configuration of the water molecules and hydrogen bonding

The five water molecules in the unit cell are located in three general positions. Water molecules W(1) and W(2) serve as apical ligands to Mn(3) and Ca respectively. As mentioned earlier, the site of the water molecule W(3), which serves as the apical ligand to Mn(4) is occupied half the time. The (OH) group serves as a common corner of the Ca polyhedron and the Mn(1) and Mn(4) octahedra (Fig. 1). The H-O-

H angles within the three water molecules, W(1), W(2) and W(3), are 108°, 102° and 126° respectively. The unusually large H-O-H angle for W(3) probably results from the large errors associated with the location of half hydrogens.

The seven crystallographically-distinct hydrogen atoms are involved in hydrogen bonding (Fig. 4 and Table 4). The (OH) group is hydrogen bonded to the oxygen atom O(11), which bridges the Si(4) and Si(5) tetrahedra. The water molecule W(1) donates one proton to the water molecule W(3) and another to O(4), an oxygen atom bridging the Si(1) and Si(2) tetrahedra. The latter hydrogen bond is rather long as well as considerably bent [W(1)-H(2)...O(4) 3.144Å, 152°]. The hydrogen atom H(4), belonging to the water molecule W(2), is probably involved in a bifurcated hydrogen bond; it is simultaneously bonded to O(1) and O(2), which bridge Si(1) and Si(5) tetrahedra, and Si(1) and Si(3) tetrahedra, respectively. The H(4)-O(1) and H(4)-O(2) distances are 2.31 and 2.44Å respectively, and the W(2)-H(4)...O(1) and W(2)-H(4)...O(2) angles are 141 and 144° respectively. Such bent bonds and long O-H...O contacts are characteristic of bifurcated hydrogen bonds. The other hydrogen atom, H(5), belonging to the water molecule W(2), is bonded to the water molecule W(1). The water molecule W(3) donates H(6) to O(9), an oxygen atom bridging the Si(3) and Si(4) tetrahedra; the other hydrogen atom, H(7), is bonded to a centrosymmetrically-related oxygen atom, O(9').

### Stereochemical configuration of the silicate double chain

#### The Si-O bond lengths and Si-O-Si angles

The average Si-O bond lengths within the Si(1), Si(2), Si(3), Si(4), and Si(5) tetrahedra are 1.621, 1.626, 1.623, 1.627 and 1.630Å respectively. The angular distortions within individual silicate tetrahedra are quite comparable, the O-Si-O angles ranging between 103° and 117°.

In terms of coordination, the oxygen atoms can be divided into five groups [cf. pyroxferroite (Burnham, 1971)]:

- A: one silicon + 3 (Mn,Ca)
- B: one silicon + 2 (Mn,Ca)
- C: two silicons + 1 Ca
- D: two silicons + 1 (or 2) H
- E: two silicons only.

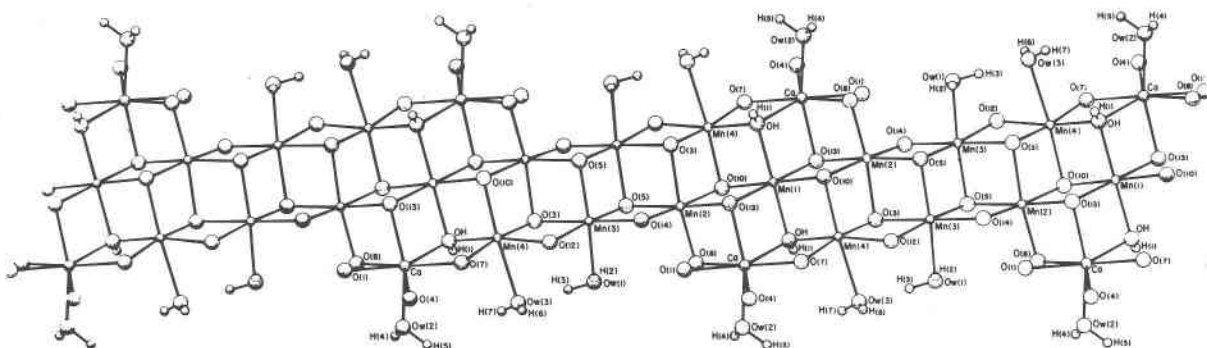


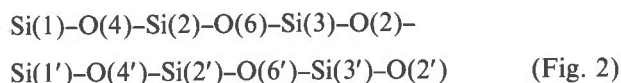
Fig. 1. Inesite: a view of the polyhedral band, showing atom nomenclature.

The average Si-O bond lengths for the A-, B-, C-, D-, and E-type bonds are 1.612, 1.592, 1.646, 1.644, and 1.628 Å respectively. As expected, the bridging bonds (C-, D- and E-types) are significantly longer than the non-bridging bonds (A- and B-types). Within the non-bridging bonds, the B-type bonds are significantly shorter than the A-type bonds, in accordance with the charge balance requirements. The D-type Si-O bonds, where the oxygen atoms are involved in hydrogen bonding, are significantly longer than the E-type Si-O bonds, where the oxygen atoms are not involved in hydrogen bonding. The D-type bridging Si-O bond lengths, where the oxygen atoms are the recipients of hydrogen bonds, are nearly the same as the C-type Si-O bond lengths, indicating the strong influence hydrogen bonds have on determining the Si-O bond lengths.

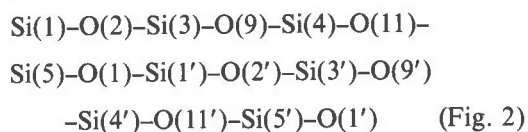
The Si-O-Si angles range from 130.5° to 143.5°, with an average of 136.0°, which is close to the average Si-O-Si angle (140°) found in a large number of silicate structures (Liebau, 1961). The smaller Si-O-Si angles are associated with larger Si-O bonds and *vice versa*, in accordance with the molecular orbital calculations on silicate chain fragments (Tossell and Gibbs, 1977). A similar correlation between Si-O-Si angles and Si-O bond lengths has been observed in zektzerite, NaLiZrSi<sub>6</sub>O<sub>15</sub>, a structure with six-tetrahedral-repeat double silicate chains (Ghose and Wan, 1978).

#### Conformation of the six-membered and eight-membered tetrahedral silicate rings

The six-membered ring has the point-group symmetry  $\bar{1}$  and the Si-O sequence:



The eight membered ring also has the point-group symmetry  $\bar{1}$ , and the Si-O sequence:



The minimum and maximum deviations of the silicon and the bridging oxygen atoms from the least-squares planes passed through the silicon atoms only are:

(a) for the six-membered ring, 0.21 and 0.26 Å (av. 0.23 Å) and 0.13 and 0.44 Å (av. 0.26 Å) respectively;

(b) for the eight-membered ring, 0.11 and 0.47 Å (av. 0.32 Å), and 0.13 to 0.48 Å (av. 0.32 Å) respectively.

The acute angle between the two least-squares planes is 9°. Hence, the double-silicate chain is slightly undulating, rather than being exactly planar.

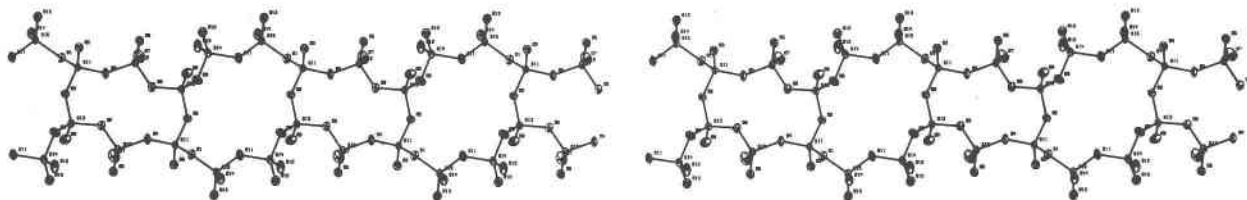


Fig. 2. A stereoscopic view of the double silicate chains with five-tetrahedral-repeat in inesite, showing ellipsoids of thermal vibration and atom nomenclature.

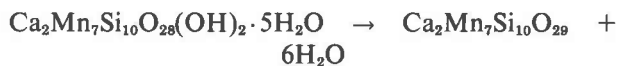
### The thermal transformation of inesite to high-calcium rhodonite

Richmond (1942) obtained nearly perfect single crystals of rhodonite by dehydrating single crystals of inesite at 800°C in a stream of nitrogen. This fact, along with the close similarity of the chemical compositions of dehydrated inesite and rhodonite, led him to believe that inesite is a hydrated form of rhodonite.

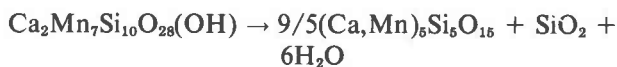
The crystal structure of rhodonite (Peacor and Niizeki, 1963; Ohashi and Finger, 1975) contains octahedral bands, formed of chains of edge-sharing octahedra, 10 octahedra long, joined in a staggered manner through further edge-sharing. The sequence within the 10-octahedra repeat band is (5-4-3-2-1-1-2-3-4-5), where 1,2,3,4,5 indicate the individual octahedral cation sites and · the symmetry center. The M(5) octahedron is slightly larger than the other octahedra, indicating a concentration of Ca in this site. However, partial occupancy of Ca in other sites (e.g., M4) is likely (Ohashi and Finger, 1975). As opposed to the 10-octahedra repeat sequence in rhodonite, a comparable 9-polyhedra repeat sequence in inesite would be 5-4-3-2-1-2-3-4-5, where 5 indicates the Ca polyhedron, and 1,2,3, and 4 the Mn octahedra: Mn(1), Mn(2), Mn(3), and Mn(4) respectively. Furthermore, rhodonite contains single silicate chains with five-tetrahedral repeat, as op-

posed to double silicate chains with five-tetrahedral repeat as found in inesite.

The dehydration reaction of inesite can be written as:



A high-calcium rhodonite with the composition  $\text{Ca}_2\text{Mn}_7\text{Si}_{10}\text{O}_{29}$ , formed by the dehydration of inesite, is deficient in one metal cation and one oxygen with respect to a high-calcium rhodonite  $\text{Ca}_2\text{Mn}_8\text{Si}_{10}\text{O}_{30}$ . In view of the structural differences between rhodonite and inesite, the thermal dehydration of inesite involves: (1) migration of metal cations to vacant octahedral sites, (2) cation disorder and partial vacancy formation around the octahedral sites, (3) breakage of Si-O bonds and migration of  $\text{Si}^{4+}$  ions to alternate tetrahedral sites, and (4) random oxygen vacancy formation around the octahedral sites coupled with cation vacancy. Alternatively, the thermal transformation of inesite to rhodonite can be represented by the reaction (Liebau, 1977, private communication):



The formation of rhodonite from inesite requires the movement of one Ca or Mn cation, which must be

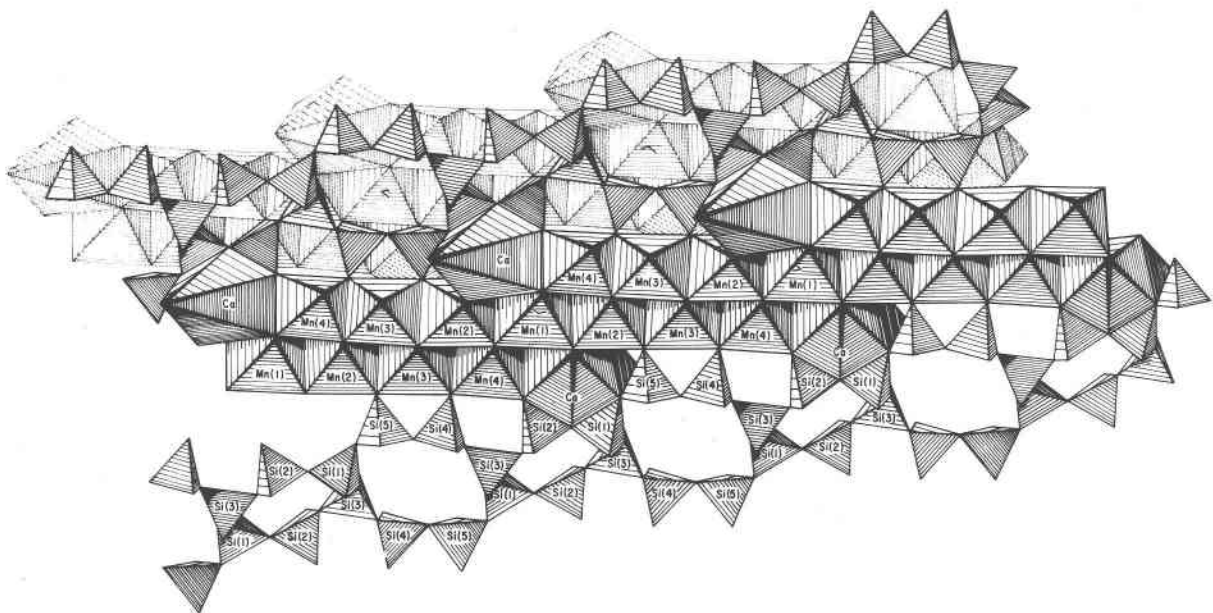


Fig. 3. A partial view of the inesite structure, showing polyhedral bands cross-linked through double silicate chains into a layer structure. Corners of the unit cell are shown; the horizontal direction in  $c \sin \alpha$ ; the other direction is  $a \sin \gamma$ .

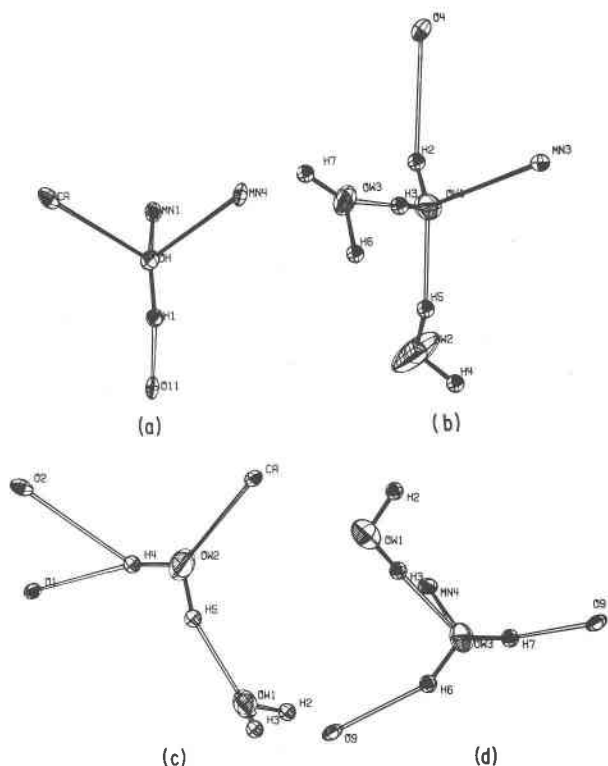


Fig. 4. Hydrogen bonding and the stereochemical configuration of the hydroxyl group and the water molecules in inesite.

provided by a part of the inesite structure. The resulting rhodonite will be free of oxygen vacancies.

In any case, the thermal transformation of inesite to rhodonite is far from a simple dehydration reaction as postulated by Richmond (1942). This pseudopolymorphic transition closely resembles the oriented thermal transformation of amphiboles to pyroxenes (Freeman and Frazer, 1968; Ghose and Weidner, 1971).

### Acknowledgments

We thank Russell Boggs, Seattle, Washington, and John S. White, Jr., Smithsonian Institution, Washington, D.C., for the donation of the inesite crystals. We are indebted to Professors Friedrich Liebau, University of Kiel, Germany, Eric Dowty, Princeton University, Yoshikazu Ohashi, University of Pennsylvania, Philadelphia, and Dr. David R. Veblen, Arizona State University, Tempe, for critical reviews of the paper. This research has been supported in part by NSF grant EAR76-13373 (Geochemistry).

### References

- Bond, W. L. (1951) Making small spheres. *Rev. Sci. Instr.*, **22**, 344–345.  
 Burnham, C. W. (1971) The crystal structure of pyroxferroite from Mare Tranquillitatis. *Proc. 2nd Lunar Sci. Conf.*, 47–57.

- Cromer, D. T. and J. B. Mann (1968) X-ray scattering factors computed from numerical Hartree-Fock wave functions. *Acta Crystallogr.*, **A24**, 321–324.  
 ——— and D. Liberman (1970) Relativistic calculation of anomalous scattering factors for X-rays. *J. Chem. Phys.*, **53**, 1891–1898.  
 Finger, L. W. (1969) Determination of cation distribution by least squares refinement of single crystal X-ray data. *Carnegie Inst. Wash. Year Book*, **67**, 216–217.  
 Freeman, A. G. and F. W. Frazer (1968) A pseudo polymorphic transition: the amphibole  $\rightarrow$  pyroxene reaction. *Nature*, **220**, 67–68.  
 Ghose, S. and C. Wan (1978) Zektzerite,  $\text{NaLiZrSi}_6\text{O}_{16}$ : a silicate with six-tetrahedral-repeat double chains. *Am. Mineral.*, **63**, 304–310.  
 ——— and J. R. Weidner (1971) Oriented transformation of grunertite to clinoferrosilite at 775°C and 500 bars argon pressure. *Contrib. Mineral. Petrol.*, **30**, 64–71.  
 Glass, J. J. and W. T. Schaller (1939) Inesite. *Am. Mineral.*, **24**, 26–39.  
 Karle, J. and I. L. Karle (1966) The symbolic addition procedure for phase determination for centrosymmetric and non-centrosymmetric crystals. *Acta Crystallogr.*, **21**, 849–859.  
 Liebau, F. (1956) Bemerkungen zur Systematik der Kristallstrukturen von Silikaten mit hochkondensierten Anionen. *Phys. Chemie*, **206**, 73–92.  
 ——— (1961) Untersuchungen über die Grösse des Si–O–Si Valenzwinkels. *Acta Crystallogr.*, **14**, 1103–1109.  
 ——— (1972) Crystal chemistry of silicon. In H.K. Wedepohl, Ed., *Handbook of Geochemistry*, II/3, 14-A-1–14-A-32. Springer-Verlag, Berlin.  
 Mamedov, K. S. and N. V. Belov (1956) Crystal structure of the minerals of the wollastonite group. I. Structure of xonotlite. (in Russian) *Zap. Vses. Mineralog. Obshch.*, **85**, 13–38.  
 Ohashi, Y. and L. W. Finger (1975) Pyroxenoids: a comparison of refined structures of rhodonite and pyroxmangite. *Carnegie Inst. Wash. Year Book*, **74**, 564–569.  
 Peacor, D. R. and N. Niizeki (1963) The redetermination and refinement of the crystal structure of rhodonite,  $(\text{Mn,Ca})\text{SiO}_3$ . *Z. Kristallogr.*, **119**, 98–116.  
 Prewitt, C. T. and D. R. Peacor (1964) Crystal chemistry of the pyroxenes and pyroxenoids. *Am. Mineral.*, **40**, 1527–1542.  
 Richmond, W. E. (1942) Inesite,  $\text{Mn}_7\text{Ca}_2\text{Si}_{10}\text{O}_{28}(\text{OH})_2 \cdot 5\text{H}_2\text{O}$ . *Am. Mineral.*, **27**, 563–569.  
 Ryall, W. R. and I. M. Threadgold (1966) Evidence for  $[(\text{SiO}_3)_6]$  type chains in inesite as shown by X-ray and infrared absorption studies. *Am. Mineral.*, **51**, 754–761.  
 Stewart, J. M., G. J. Kruger, H. L. Ammon, C. Dickinson and S. R. Hall (1972) The X-RAY SYSTEM—version of June 1972. *Tech. Rep. Tr-192*. Computer Science Center, University of Maryland, College Park, Maryland.  
 Tossell, J. A. and G. V. Gibbs (1977) Prediction of T–O–T angles from molecular orbital studies on cornersharing mineral fragments (abstr.). *Trans. Am. Geophys. Union*, **58**, 522.  
 Wan, C. and S. Ghose (1975) Inesite,  $\text{Ca}_2\text{Mn}_7\text{Si}_{10}\text{O}_{28}(\text{OH})_2 \cdot 5\text{H}_2\text{O}$ : a new chain silicate with “Fünferdoppelketten.” *Naturwissenschaften*, **62**, 96.

Manuscript received, July 22, 1977; accepted for publication, January 8, 1978.